BMC Microbiology

RESEARCH Open Access

Characterization of a novel lytic phage vB_AbaM_AB4P2 encoding depolymerase and its application in eliminating biofilms formed by *Acinetobacter baumannii*

Jianhui Su[1†], Yujing Tan[1†], Shenshen Liu[1†], Huanhuan Zou[1], Xiaoyi Huang[1], Siyi Chen[1], Hongmei Zhang[1], Shaoting Li[1] and Haiyan Zeng[1*]

Abstract

Background *Acinetobacter baumannii* strains are a primary cause of hospital-acquired infections. This bacterium frequently causes biofilm-related infections, notably ventilator-associated pneumonia and catheter-related infections, which exhibit remarkable resistance to antibiotic treatment, posing a severe challenge in the prevention of *A. baumannii* infections. Therefore, strategies to eliminate the biofilm of *A. baumannii* in catheters are becoming increasingly important. Phages are capable of lysing bacteria and have a certain effect on the ablation of biofilms.

Methods Sewage treatment plant water was collected for the isolation of *A. baumannii* phages. The morphological, host range, one-step growth, temperature and pH stability, bactericidal activity, sequencing and genomic analysis were performed to characterize the isolated phage. The three-dimensional structure of the tail fiber protein was predicted by AlphaFold3. The efficacy of phage in clearing biofilms of *A. baumannii* from 24-well plates and PVC catheters was also evaluated.

Results In this study, *A. baumannii* lytic phage vB_AbaM_AB4P2 was isolated from sewage treatment plant water, showing a clear plaque with halo zone. One-step growth assays unveiled a 20-minute latent period and a burst size of 61 plaque forming unit/cell (PFU/cell). At the same time, phage AB4P2 exhibited remarkable stability at pH 3–11 and temperatures 30–70 °C. Its dsDNA genome is composed of 45,680 bp with a G + C content of 46.13%. Genomic and phylogenetic analysis situated phage AB4P2 as a new species of *Caudoviricetes* class. Its fiber protein possesses a pectin lyase-like domain that is linked to depolymerase activity, playing a crucial role in disrupting biofilms. Additionally, it also encodes a lysis cassette comprising endolysin, holin and Rz-like spanin, yet lacks any genes responsible for antibiotic resistance and virulence factors. Phage AB4P2 can completely inhibit *A. baumannii* growth

†Jianhui Su, Yujing Tan and Shenshen Liu contributed equally to this work.

*Correspondence:
Haiyan Zeng
zenghy@aliyun.com; zenghy@gdut.edu.cn

Full list of author information is available at the end of the article

for 16 h. In the 24-well plate and the polyvinyl chloride (PVC) catheter model experiments, phage AB4P2 achieved a significant biofilm ablation rate and effectively killed the live bacterial cells in the biofilm.

Conclusions Phage AB4P2 had good environmental stability and strong ability to inhibit the growth of *A. baumannii* and destroy formed biofilms by *A. baumannii*. It exhibits promising potential for development as an alternative environmental disinfectant against *A. baumannii* in the hospital.

Clinical trial number Not applicable.

Keywords *Acinetobacter baumannii*, Phage, Genome, Depolymerase, Biofilm, Catheter

Background

Acinetobacter baumannii is a conditionally pathogenic bacterium and a significant nosocomial pathogen that plagues healthcare facilities [1]. It predominantly incites respiratory tract infections but also can instigate bloodstream infections, urinary tract infections, secondary meningitis, surgical site infections, and ventilator-associated pneumonia, among other maladies [2]. In the previous decade, the infection rates of *A. baumannii* have gradually increased in the hospital, and the majority of *A. baumannii* infections manifest in the Intensive Care Unit (ICU) (with isolation rates exceeding 70%) [3]. The formation of biofilms on abiotic surfaces is a key factor in the etiology of medical device-associated infections, as it facilitates the persistence of *A. baumannii* in healthcare settings, particularly on medical devices and within the ICU environment. Additionally, biofilms diminish the bactericidal effectiveness of common disinfectants, including benzalkonium chloride and ethanol [4]. *A. baumannii* frequently causes biofilm-related infections, particularly ventilator-associated pneumonia and catheter-related infection, which can be exceedingly resistant to antibiotic therapy, offering a severe challenge to prevent *A. baumannii* infection [3]. Therefore, strategies to eliminate the biofilm of *A. baumannii* in medical devices and catheters are becoming increasingly important.

Phages are the most widely encountered organisms that are natural bacterial killers, and have been used in practical application since the early 20th century [5, 6]. The phage therapy offers notable advantages, being adept at disrupting biofilms and eliminating targeted bacterial strains without significantly disrupting the human microbiota's balance [7]. As natural enemies of bacteria, phages can eradicate biofilms through several mechanisms and act on the target bacterial cells. One of the most crucial mechanisms is that phages can encode a variety of enzymes, such as depolymerases and lysins, to break down the defense barrier during infections of the host bacteria [3, 8]. Endolysins play a crucial role by degrading bacterial cell walls at the culmination of the phage replication cycle, thereby releasing newly formed phage particles [5, 8]. It was reported to reduce biofilm formation against host bacteria [8]. Phage-encoded depolymerases include two main classes: hydrolases and lyases, which are used to facilitate initial stages of the phage infection cycle (adsorption and DNA injection) [9, 10]. Depolymerases can degrade polymers [11], either associated with capsule polysaccharides (CPS) in the cell surface to enhance phage adsorption, or extracellular polymeric substances (EPS) produced in the biofilm in order to promote phage diffusion through the bacterial slime [9, 12, 13]. As a result, the phage with depolymerase was able to efficiently kill biofilm cells and, at the same time, degrade the biofilm EPS matrix [9, 14]. This process not only increases bacterial sensitivity to phage therapy but also facilitates the treatment of bacterial infections and the targeted removal of bacterial biofilms from medical devices [5, 8, 15].

Phage therapy has excellent effects and advantages, yet its application is still constrained by several limitations, such as the narrow host range, phage resistance, delivery challenge, the lysogenic phenomenon, the lack of relevant policies, and the lack of pharmacokinetic data [16–18]. At the same time, there exists a conspicuous dearth of highly lytic and comprehensively characterized phages available for application, a shortfall exacerbated by the mounting demand for their utilization [5, 19]. In response to this exigency, we performed the isolation of *A. baumannii* lytic phages from sewage treatment plant water, and delved into the identification and biological characteristics analyses of the new lytic *A. baumannii* phage vB_AbaM_AB4P2 (abbreviated as phage AB4P2) which have a depolymerases activity. Then we evaluated the biofilm ablation effect of *A. baumannii* by phage AB4P2 in 24 well plate. What's more, *A. baumannii* biofilm model of PVC catheter was developed and applied to evaluate the ability of phage AB4P2 to remove biofilms.

Materials and methods

Phage isolation and transmission electron microscopy (TEM)

The *A. baumannii* strains used in the present study were isolated from clinical samples in Guangzhou. Luria-Bertani (LB) broth and LB agar were used to cultivate these strains. The water samples were collected from a sewage treatment plant in Luoyang city. *A. baumannii* strain AB4, identified through the automated VITEK 2 Compact system (bioMérieux, Marcy l'Etoile, France),

was used as the host for phage isolation. The isolation of phage was performed according to our previously described method [20]. The pure bacteriophages were obtained by at least four single-plaque isolations, The purified phage was applied to carbon-coated copper grids, and excess liquid was removed using filter paper. A 5% solution of photosensitive acid was prepared using ddH_2O as the solvent. Negative staining was achieved by exposing the bacteriophage to 5% phosphotungstic acid (pH = 6.7) for one minute. Prepared samples were scrutinized under a Transmission Electron Microscope (TEM; Hitachi HT7700, Japan) [21]. The bacteriophages were stored at 4 °C in LB broth for further use and − 80 °C in 30% glycerol and SM preservation solution (200mM $NaCl_2$, 10mM $MgSO_4$, 50mM Tris-HCl, pH 7.5) respectively for long-term preservation. The phage vB_AbaM_AB4P2 (hereafter referred to as phage AB4P2) forming a clear plaque with halo zone was selected for further experiments.

Host range, multiplicity of infection (MOI) and one-step growth experiment

The host range of *A. baumannii* phage AB4P2 was assessed against 24 different strains, including 7 *A. baumannii*, 5 *Escherichia coli*, 2 *Pseudomonas aeruginosa*, and 10 *Salmonella* strains (Supplemental Table 1). Phage AB4P2 was capable of forming plaques on *A. baumannii* AB3 and AB4. Briefly, 100 µL of bacterial liquid in the log phase was mixed with 5 mL of soft LB (0.7% agar) and then poured onto the bottom LB plate (1.5% agar). After standing for 15 min at room temperature, 10 µL of phage liquid was spotted onto the soft agar. The plates were incubated at 37 °C for 10-12 h. The transparent phage plaque can be observed if this phage can lysis the host strain.

The MOI was performed according to our previously reported method with minor modification [22]. The phages were purified by One-step salting-out extraction [23]. Based on the ratios of 10, 1, 0.1, 0.01, 0.001, 0.0001 (phage to bacteria), plus 1 ml of host strain cells and 1 ml of serially diluted phages were mixed and shaken at 37 °C for 4 h at 200 rpm and centrifuged at 12,000 rpm for 10 min. The supernatant was filtered through a membrane with 0.45-µm pores. The one with the highest phage titers was the optimal MOI. Three parallel experiments were performed.

One-step growth experiment was performed according to our previously reported method (20). The optimal MOI 1 was employed to incubate the mixture at 37 °C for 5 min. Subsequently, the mixture was centrifuged at 12,000 g for 30 s to remove unabsorbed free phages. Following two washes, precipitated cells were resuspended in 10 mL of LB broth supplemented with 2 mmol/L $CaCl_2$ and subjected to shaking at 37 °C and 200 rpm. The experiment was initiated at t = 0, with subsequent time points defined at t = 0, 10, 20, 30, 40, 50, 60, 70, 80, 90, 120, 130, and 180 min. Phage titers were determined using the double-layer agar method. The experiment was repeated three times.

Stability of phage at different temperatures and pH

To evaluate thermal stability, the phage AB4P2 preparation (1×10^9 PFU/mL) was subjected to LB at temperatures ranging from 30 °C to 70 °C for 1 h. Meanwhile, to assess its pH stability, the phage preparation (1×10^9 PFU/mL) was exposed to pH levels ranging from 2 to 12 for 1 h. The pH of LB was adjusted using NaOH and HCl solutions before cultivating phages. The stability of bacteriophages was determined by changes in phage titer. Three parallel experiments were performed to determine the stabilities of the phage preparations, and phage titers were determined using the double-layer agar technique [24].

Genome sequencing and bioinformatics analysis

Phage AB4P2 DNA was extracted according to our previously reported method [20]. The genomic DNA was sent to Guangdong Meigi Gene Technology Company, Limited, and subjected to whole-genome sequencing using MiSeq (Illumina, CA, USA), and filtered data were assembled with the SPAdes (v3.6.2) program [25]. Gene annotation was conducted using Pharokka, and the putative protein function of the open reading frames (ORFs) were annotated using BLASTp against the Non-Redundant Protein Database of the NCBI. Searches for antibiotic resistance genes and virulence genes were performed using ResFinder 2.1 (https://cge.cbs.dtu.dk/services/ResFinder-2.1/) and the virulence factor database (http://www.mgc.ac.cn/VFs/), respectively. The genome was sub jected to comparisons with other nucleotide sequences using NCBI BLASTn (https://blast.ncbi.nlm.nih.gov/Blast.cgi). The classification prediction of phages was carrie d out using PhaGCN2.0 [26]. The construction of a phylogenetic tree, based on whole-genome sequences of the phage isolated in this study and other reported prokaryotic dsDNA viruses, was accomplished using ViPTree [27]. Average nucleotide identity (ANI) calculation and their heatmap were generated using pyani (https://github.com/widdowquinn/pyani). Nucleotide-based intergenomic similarities of phages were calculated by VIRIDIC [28]. The genomic architecture of similar bacteriophages was compared using Easyfig 2.23 [29]. InterPro was employed to annotate the functional domains of tail proteins [30]. The 3D structure of tail fiber proteins was predicted by AlphaFold3 [31] and visualized by. Structural analyses and visualizations were performed with PyMOL [32].

Effect of the phage on the growth of the host bacteria

Total 100 µL of *A. baumannii* strain AB4 (10^7 CFU/mL) was mixed with 100 µL of phage AB4P2 solution (optimal MOI). The mixture was incubated at 37℃ for 24 h. The lytic capacity was determined by measuring the OD600 at 1 h intervals using Bioscreen C MBR (MGC-200PRO, China). The positive control group was prepared by mixing 100 µL of host bacteria with 100 µL of LB broth, while the negative control group consisted of 100 µL of phage solution mixed with 100 µL of LB broth [22].

Ablation effect of bacterial biofilm on a 24-well plate

A. baumannii was cultured to early log phase and seed bacterial (900 µL, 10^7 CFU/mL) onto a 24-well plate and incubate at 37 °C for 48 h incubation. The medium of plates were discarded and then washed twice with phosphate buffered saline (PBS). The phage AB4P2 lysate (100µL, 10^9 PFU/mL) was added to the 24-well plate, then cultured at 37 °C for 2 h. The wells were washed twice using PBS and dried in room temperature. Crystal violet (CV) at a concentration of 0.1% was used to stain the adhered bacteria before being rinsed two with PBS. The CV-stained wells received 0.3 mL of acetic anhydride (33%) for the quantification of biofilm growth, which was then incubated with shaking for 2 h. At 590 nm, optical density was measured [33]. The control group was prepared by mixing 900 µL of host bacteria with 100 µL of LB broth, while the blank group consisted of 1000 µL of LB broth. *A. baumannii* (10^7 CFU/mL) was added to a tissue culture dish and incubated for 48 h to cultivate biofilms. After that, PBS, phage (10^8 PFU/mL) were supplemented and incubated at 37 °C for 2 h. Then *A. baumannii* was stained with Live-Dead Cell Staining Kit (beibokit, China) and observed by fluorescence inverted microscope (Life Technologies, EVOS FL Auto, China). The biofilm inhibition (%) was calculated using the following formula: Biofilm ablation (%) = {[(OD590 $nm_{control}$– OD590 nm_{blank})– (OD590 $nm_{treatment}$–OD590 nm_{blank})]/(OD590 $nm_{control}$– OD590 nm_{blank})}× 100.

Application in the ablation of biofilms on Polyvinyl chloride (PVC) catheters

The PVC catheter was submerged in a bacterial solution and incubated for 37 °C for 48 h. PVC catheter mimics were flushed twice with sterile LB broth. The catheter was then submerged in 5 mL phage AB4P2 lysate at a titer of 1×10^7 PFU/mL for 2 h. The PVC catheter mimics were flushed three times with sterile PBS. Catheter mimics were then air-dried for 10 min and 300 µL of 0.1% CV stain was pipetted into the lumen of the catheter mimic containing the biofilm and left for 10 min. Catheter mimics were then flushed three times with 1 mL of diH2O. Images of stained catheter mimics were taken prior to solubilizing the CV stain. The CV-stained wells received 0.3 mL of acetic anhydride (33%) for the quantification of biofilm growth, which was then incubated with shaking for 2 h. At 590 nm, optical density was measured. For the control, LB broth was used instead of the phage lysate. For the blank, LB broth was used instead of the bacterial solution and phage lysate. The experiments were repeated three times [34, 35]. The calculation of biofilm ablation (%) is the same as before.

Statistical analysis

The statistical analyses were determined by the one-way ANOVA test of GraphPad Prism (v6, GraphPad Software Inc., CA, USA). The difference thresholds were set at $p < 0.05$ and $p < 0.01$.

Results

Phage isolation, morphology, and host range profile

Total 29 phages were isolated from sewage treatment plant water. Among these phages, phage AB4P2 formed clear plaques with a diameter of 4 mm with halo zones approximately 10 mm in diameter on a bacterial lawn of the host strain *A. baumannii* AB4 (Fig. 1a). The halo zones observed in the plaques of phage AB4P2 suggested that it had the ability to depolymerize exopolysaccharides and biofilms. The TEM result of phage vB_AbaM_AB3P2 particles reveal that it had an icosahedral head with diameter of approximately 80 nm, and a tail with a length of about 100 nm (measured by 10 phage particles) (Fig. 1b).

Growth and stability of phage AB4P2

Phage AB4P2 exhibited its maximum titer of 6.8×10^9 PFU/ml when the MOI was set to 1 (Fig. 1c). The one-step growth curve experiment (Fig. 1d) unveiled a latent period of approximately 20 min, followed by an exponential growth phase over the subsequent 110 min. The calculated burst size of phage AB4P2 was approximately 61 PFU/cell. To evaluate the stability of phage AB4P2 under different environmental conditions, experiments were conducted at various temperatures and pH values. The phage exhibited remarkable thermal tolerance, remaining stable at temperatures ranging from 30 °C to 70 °C (Fig. 1e). At the same time, the phage titer remained stable in the pH range of 3–11 (Fig. 1f), however, it lost its activity lower than pH 2 and higher than pH 12.

Genomic and phylogenetic analysis of phage AB4P2

The genome of phage AB4P2 was found to consist of a dsDNA molecule measuring 45,680 bp in length, with a G + C content of 46.13%. A total of 90 open reading frames (ORFs) were identified within the genome, with 44 out of 90 (48.9%) annotated genes associated with various phage functions, including phage structure (head protein, tail protein, portal protein), lysis protein,

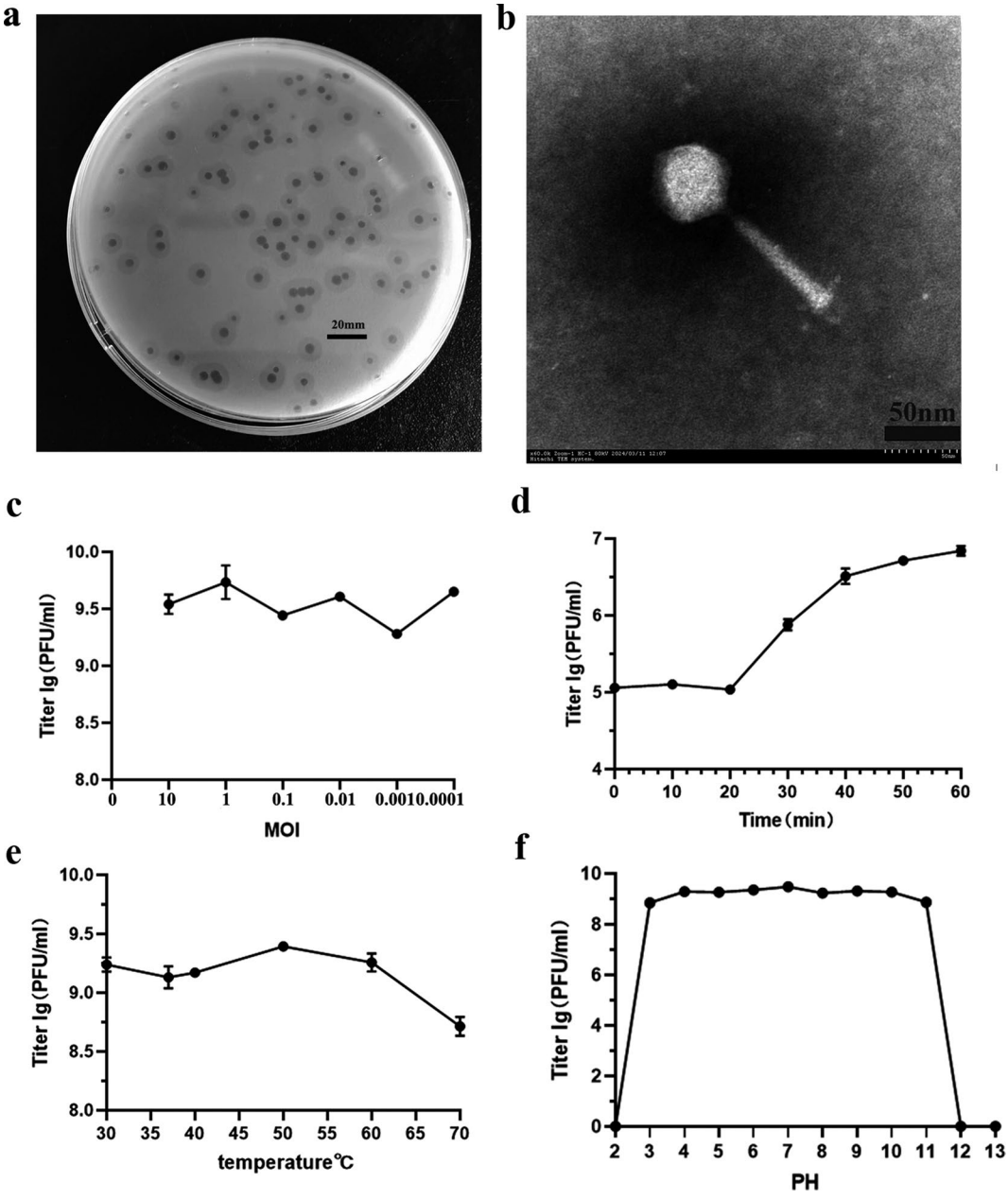

Fig. 1 Morphological and biological characterization of *Acinetobacter baumannii* phage vB_AbaM_AB4P2. (**a**) *A. baumannii* phage vB_AbaM_AB4P2 plaques. (**b**) Morphology of *A. baumannii* phage vB_AbaM_AB4P2 presented by transmission electron microscopy (TEM). (**c**) Optimal multiplicity of infection (MOI) determination. (**d**) One-step growth curve. (**e**) Stability of *A. baumannii* phage vB_AbaM_AB4P2 at different temperatures. (**f**) Stability of *A. baumannii* phage vB_AbaM_AB4P2 at different pH

transcriptional regulators, and metabolism. Notably, no rRNA, tRNA, antibiotic resistance genes, or virulence genes were detected.

BLASTn analysis against the NCBI non-redundant database revealed that the sequence most similar to phage vB_AbaM_AB4P2 was from *Salmonella* phage IME207 [36], with an identity of 92.58% and coverage of 65%. A viral proteomic tree based on whole-genome sequences of phage vB_AbaM_AB4P2 and all phages in VipTree database ($n = 5633$) were constructed (Fig. 2a). Further, all the phages in the cluster comprising phage AB4P2 and other phages were selected to regenerate a new phylogenetic tree ($n = 20$). As shown in Fig. 2b, all of these phages belonged to different genus of *Caudoviricetes* class. Moreover, phage vB_AbaM_AB4P2 showed a relatively closer relationship with *Salmonella* phage vB_Se_STGO-35-1 which belonged to *Caminolopintovirus* genus. *Salmonella* phage IME207 which had the highest identity with this phage by BLASTn was located in another small cluster showing a comparatively distant

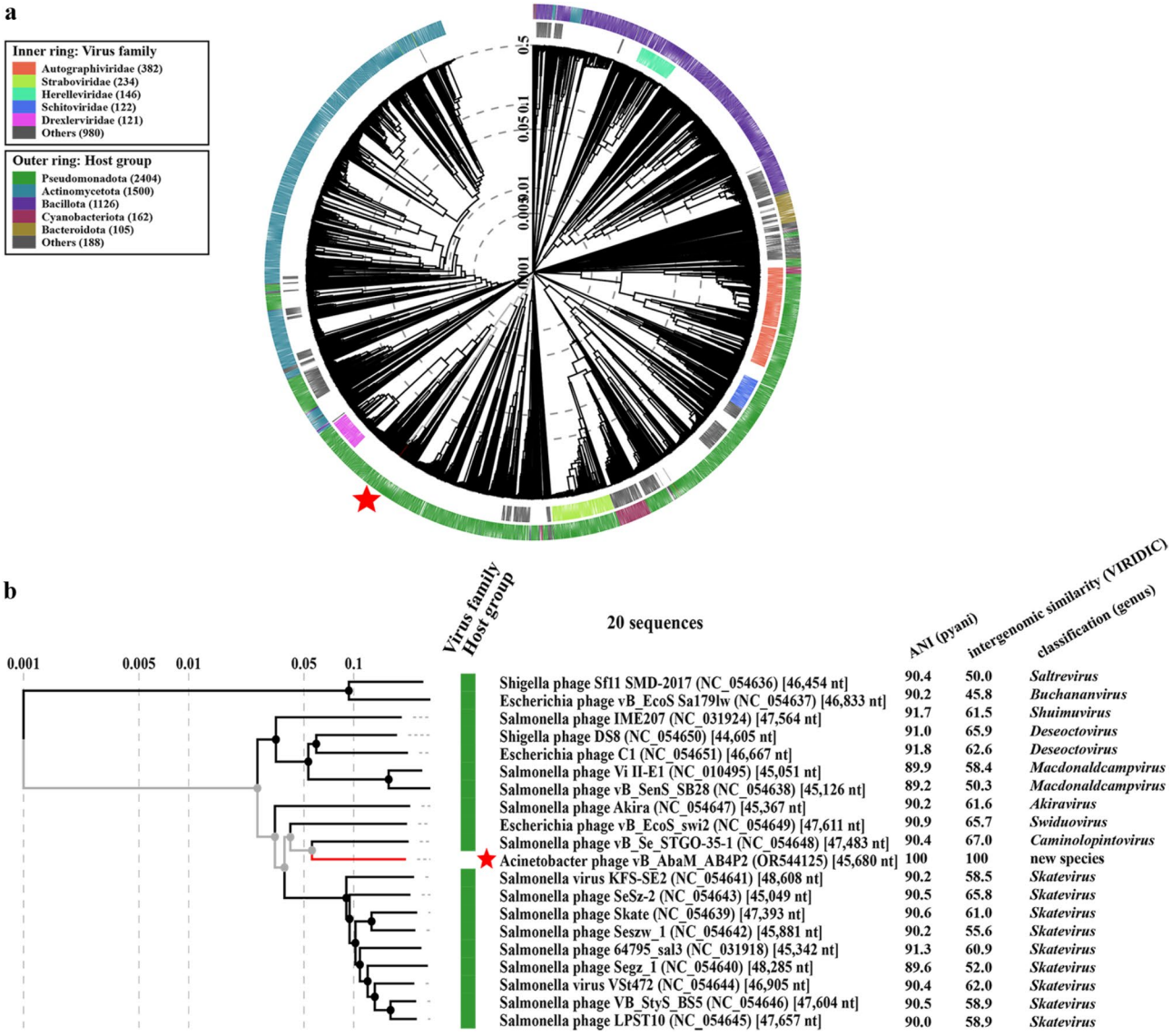

Fig. 2 Phylogenetic tree based on phage whole genome sequences using ViPTree. (**a**) A viral proteomic tree based on whole-genome sequences of phage vB_AbaM_AB4P2 and all related phages ($n = 5663$). Phages are identified according to their official ICTV classification, with the outer and inner rings representing their host group and the family level, respectively. Unmarked phages have not been classified to existed family yet. Phage vB_AbaM_AB4P2 is indicated by star. (**b**) A regenerated tree based on all the phages in the cluster comprising phage vB_AbaM_AB4P2 and other related phages ($n = 20$). The ANI value calculated by pyani and the intergenomic similarity value by VIDIRIC between the specific phage and vB_AbaM_AB4P2, and the classification information were shown in the right next to the corresponding phage

phylogenetic relationship. The ANI analysis of these 20 phages showed that phage vB_AbaM_AB3P2 was most similar to *Escherichia* phage C1 (91.8%) (Fig. 2b and Supplemental Fig. 1), the intergenomic similarity analysis indicated that it was most similar to *Salmonella* phage vB_Se_STGO-35-1 (67.0%) (Fig. 2b and Supplemental Fig. 2).

Moreover, genome colinear comparisons with highly similar phages, *Salmonella* phage IME207 (with the highest identity by BLASTn), *Escherichia* phage C1 (with the highest identity by pyani) and *Salmonella* phage vB_Se_STGO-35-1 (with the highest intergenomic similarity by VIRIDIC and the closet phylogenetic relationship by VIPTree), indicated several differences among these phages (Fig. 3a). All four phages possessed a lysis cassette including two endolysins, one holin and one Rz-like spanin. These observations highlighted the strong lytic activity of these phages and the variations between them, including differences in tail proteins. Especially, the tail fiber protein (WPJ20733) of phage AB4P2 was different from that of other phages. As shown in Fig. 3b, the pectin lyase-like domain exhibiting a right-handed parallel β-helix structure was observed in this tail fiber protein. This domain plays a key role in specifically recognizing and degrading

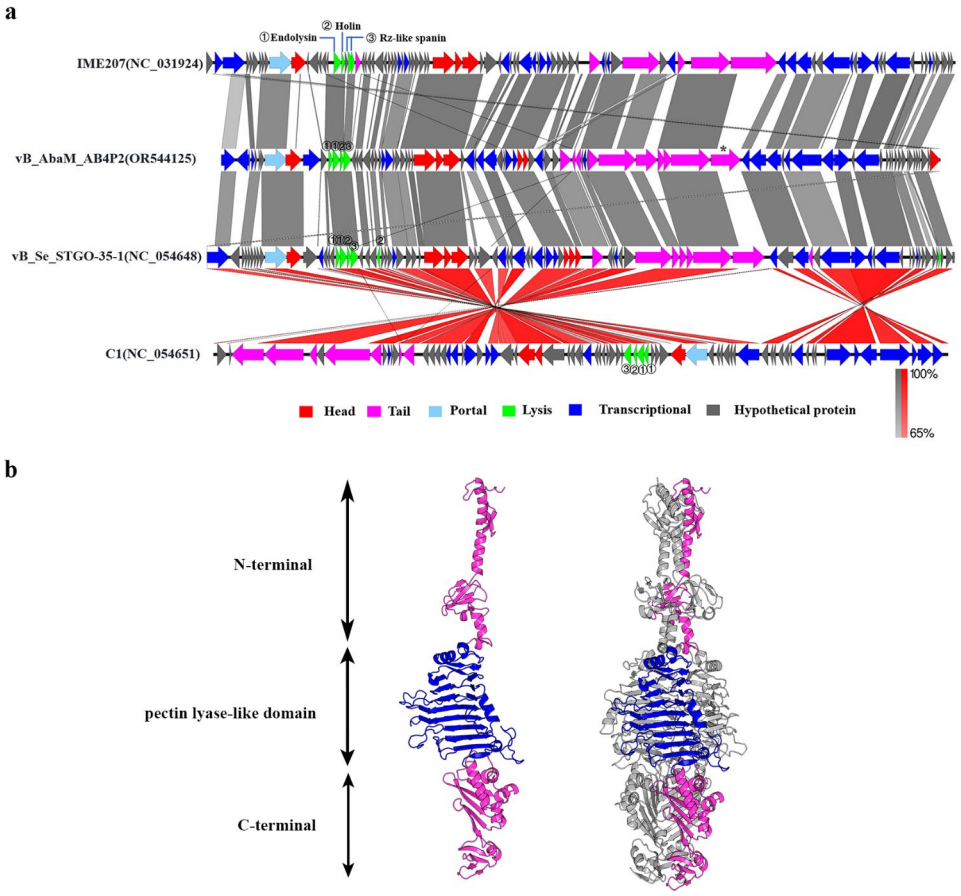

Fig. 3 The genomic structure of *A. baumannii* phage vB_AbaM_AB4P2 and its functional domain responsible for depolymerase activity. (**a**) Schematic genomic alignment with *Salmonella* phage IME207, *Salmonella* phage vB_Se_STGO-35-1, and *Escherichia* phage C1 generated using EasyFig. The bar in the lower right corner shows the identity percentage for normal and inverted BLAST matches. (**b**) 3D structural analysis of the tail fiber protein WPJ20733 in phage vB_AbaM_AB4P2. The structure of this protein, predicted using AlphaFold3, is shown in both its monomeric form (left) and trimeric assembly (right). The pectin lyase-like domain (colored in blue) adopts a right-handed parallel β-helix structure, which is crucial for substrate binding and catalytic activity

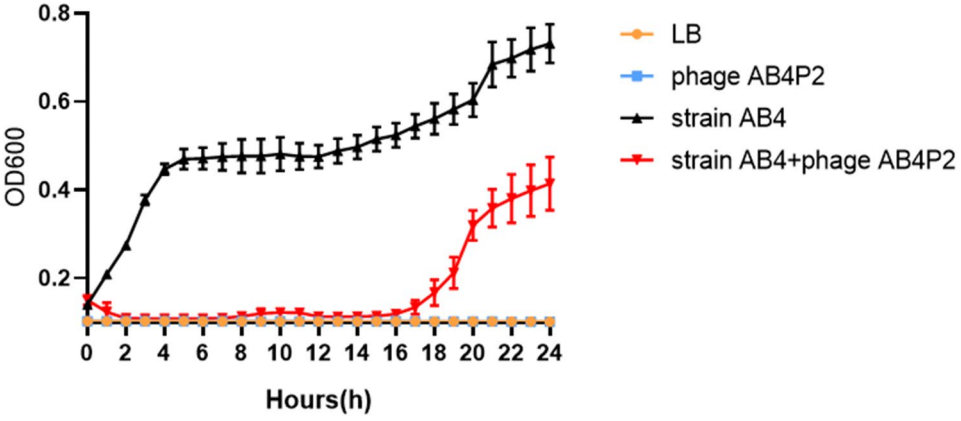

Fig. 4 Growth inhibition of *A. baumannii* by phage vB_AbaM_AB4P2

exopolysaccharides within biofilms, as well as the bacterial capsular polysaccharide of host bacteria [37, 38]. This domain is thought to be associated with depolymerase function [39].

Growth Inhibition of *A. baumannii* by phage AB4P2

As shown in Fig. 4, A. *baumannii* AB4 exhibited rapid growth within the initial 0 to 4 h period, transitioning into the stationary phase by the fifth hour. The impact

of the phage was evident as it completely inhibited the growth of the AB4 strain within a 16-hour timeframe [22]. Although the growth of the strain was slightly resumed later, it remained significantly lower compared to the non-phage control. This result indicated phage AB4P2 had a highly efficient antibacterial ability.

Bacterial biofilm ablation of *A. baumannii* by phage AB4P2

Bacterial biofilms display obvious resistance against disinfect the environment and are largely implicated in chronic and intractable infections [8]. Effectively eliminating biofilms is essential for the prevention of clinical infections. The effectively eradicate existing biofilm by phage AB4P2 was observed in Fig. 5A, the phage AB4P2-treated groups exhibited significant ablation effects on the biofilm compared with the control groups, and the biofilm ablation rate was 52% [40]. To further evaluate the antibiofilm activity of phage AB4P2, the mature bacterial biofilms were observed by fluorescence inverted microscope. As shown in Fig. 5B, following phage AB4P2 treatment, the dead bacterial cells in biofilm were significantly increased. This observation suggests that phage AB4P2 had effectively killed the live bacterial cells in the biofilm [41]. In combination with the crystal violet and fluorescence staining methods, the study demonstrated that phage AB4P2 was capable of effectively ablating biofilms.

Ablation effect of *A. baumannii* biofilm on PVC catheters

This study aimed to evaluate the efficacy of phage AB4P2 in eliminating luminal biofilms on catheters, employing a PVC catheter mimic biofilm model as outlined in the methods section. Visualization of the control catheter mimics post-crystallization with CV revealed a distinct

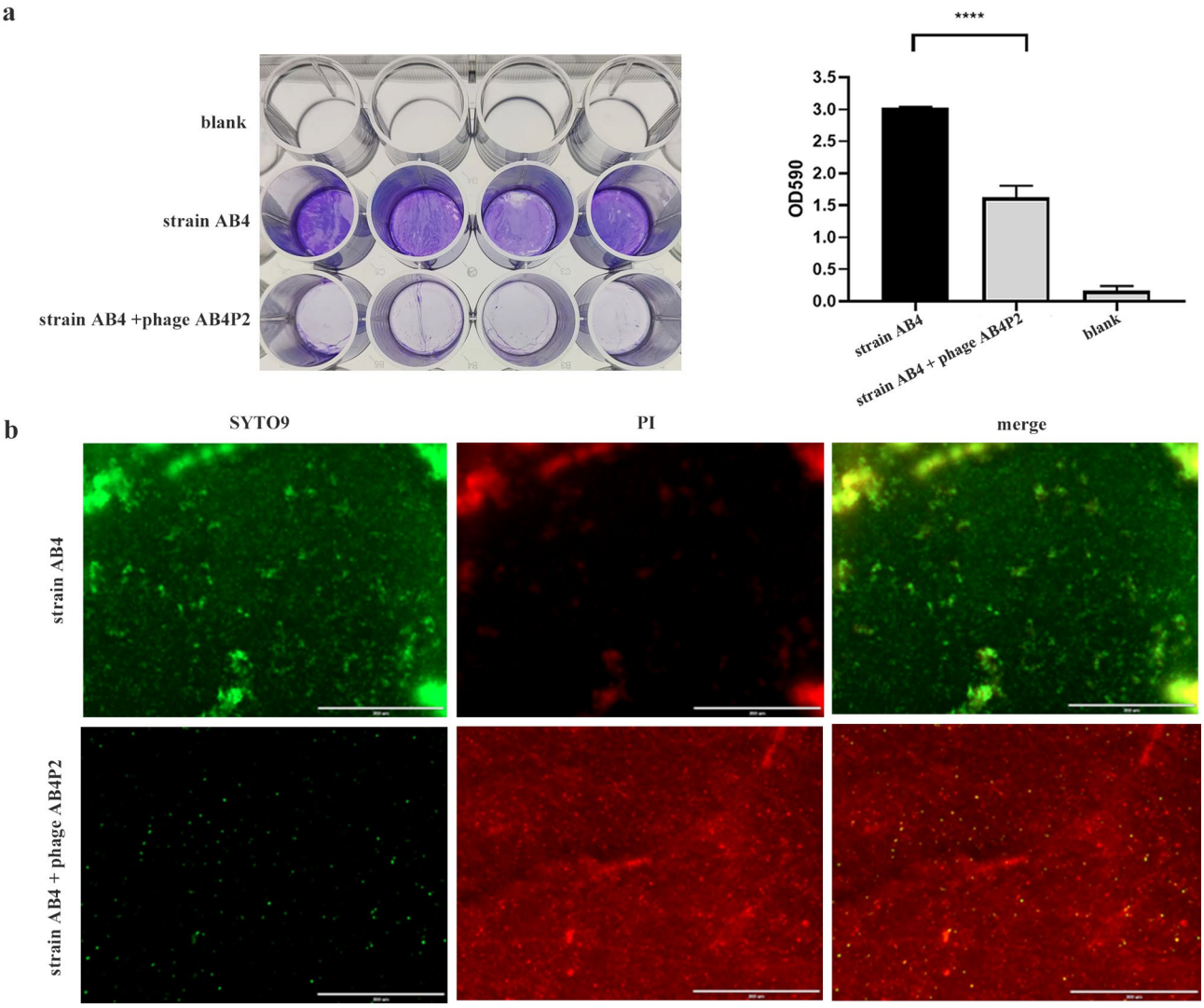

Fig. 5 Biofilm ablation of *A. baumannii* by phage vB_AbaM_AB4P2. (**a**) Crystal violet staining images of samples in 24 well plate and their OD590 values. (**b**) Live/dead bacterial viability test by fluorescence microscope. (green: live) (red: dead)

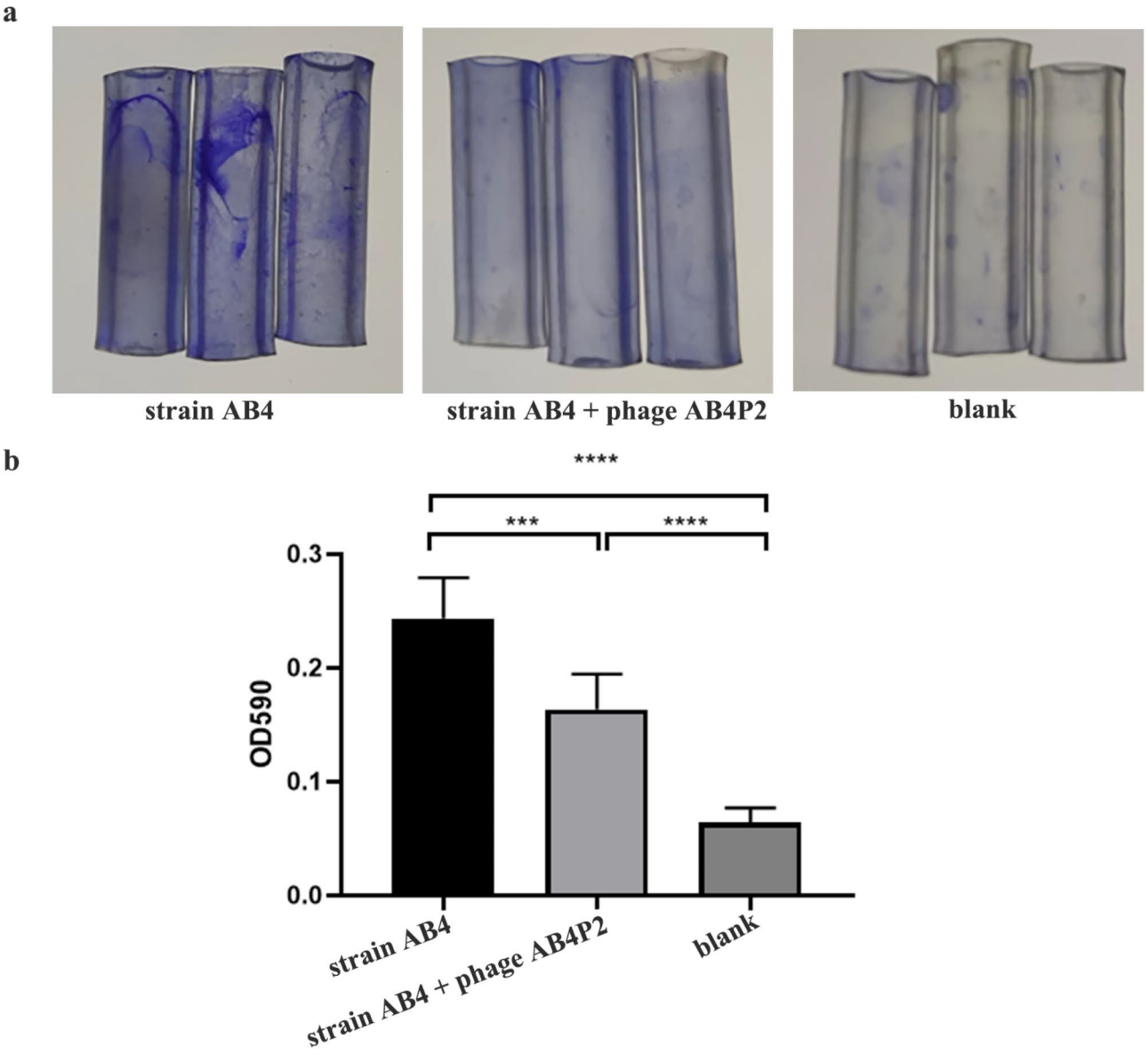

Fig. 6 Application of phage vB_AbaM_AB4P2 for the removal of *A. baumannii* biofilm on PVC catheters. (**a**) Crystal violet staining images of samples on PVC catheters and (**b**) the OD590 value of samples

purple-stained region at the center of the mimic (Fig. 6a), which confirms that the biofilm matrix remained intact throughout the preparation process, with no significant loss of biofilm material. The treated catheter exhibited a marked reduction in large biofilm formations, with the internal biofilm layer notably thinning in comparison to the catheter that remained untreated, indicating that the phage treatment effectively removed the entire biofilm in the targeted region (Fig. 6a) [34]. The blank control group exhibited notable differences when compared to the other two groups, demonstrating that the absence of purple coloration on the catheter was indicative of no bacterial attachment. Solubilizing the CV stain and analysis with spectrophotometry revealed quantifiable biofilm signals (Fig. 6b). The mean value of OD590 in catheter mimic control groups was 0.24 with a standard deviation of 0.035, in phage treated catheter mimic group was 0.16 with a standard deviation of 0.031, in LB blank groups was 0.06 with a standard deviation of 0.012. The data revealed that phage therapy led to a substantial 33% decrease in the biofilm within a two-hour treatment. Statistically significant differences between treated and untreated groups (p value < 0.05) were observed.

Discussion

A. baumannii is recognized as a clinically significant pathogen causing a wide spectrum of nosocomial infections. In this study, we isolated one lytic *A. baumannii*

phage AB4P2 from a sewage treatment plant in China. The current criterion for defining new species of bacteria and archaeal viruses is set at a genome identity of 95%. The identity, ANI and intergenomic similarity between phage AB4P2 and all similar phages were less than 95%, in addition with the global genomic differences identified through collinear comparison among these highly similar phages, all these results supported that phage AB4P2 was a novel species (Figs. 2 and 3). Due to the result that the three most similar phages to phage AB4P2, *Salmonella* phage vB_Se_STGO-35-1, *Salmonella* phage IME207, and *Escherichia* phage C1, belong to different genera of *Caudoviricetes* class, it is impossible to determine the genus of this new phage (Fig. 2). *Caudoviricetes* class encompasses 7 orders, 74 family, 121 subfamily, 1497 genera and 4840 species. Nevertheless, phage AB4P2 does not fit into any of these established classifications, it is a novel species of *Caudoviricetes* class.

Environmental factors can affect phage stability, consequently reducing the efficacy. In previous studies, the activity of *A. baumannii* phages ϕAbp2 [24], sharply decreased at PH = 4.0 and PH = 11.0, the titers of *A. baumannii* phage pIsf-AB02 and the phage vB_AbaS_TCUP2199 were slightly dropped at 50 °C and reduced dramatically at 70 °C, the phage vABWU2101 had a survival rate of 60% at 60 °C, but became inactive at 70 °C [42–44]. In this study, phage AB4P2 was stable in pH 3–11 and 30–70 °C, showing an advantage under acid stress and high temperature. Genomic analysis showed that the phage AB4P2 genome did not contain any genes related to rRNA, tRNA, antibiotic resistance genes, or virulence factors, qualifying it for further application. Moreover, phage AB4P2 had a lysis cassette, including two endolysins, one holin and one Rz-like spanin (Fig. 3). These lytic proteins were necessary for the lysis of gram-negative bacteria by *Caudoviricetes* phages. The presence of these lysis proteins implied that this phage had a strong lysis ability. We investigated the potential ability of phage AB4P2 to eliminate *A. baumannii* in LB broth (Fig. 4), and found that the growth of host bacterial cells was completely inhibited as early as 16 h after treatment with the phage. However, most phages can only inhibit bacterial growth within 12 h, such as phage SLAM_phiST1N3 and vB_PaeP_TUMS_P121 in previous studies [45, 46].

The capacity of *A. baumannii* to form biofilms on both biotic and abiotic surfaces is a critical factor that underpins the chronicity and persistence of infections, antimicrobial resistance, and robust survival in healthcare settings [47]. The elevated prevalence of *A. baumannii* infections associated with medical devices is largely attributed to the formation of biofilms, which significantly complicates efforts in treatment and infection control [47]. Phages have the ability to infiltrate biofilm layers via natural pores and channels, leading to the subsequent disruption of the biofilm matrix [9, 48]. These viruses encode a diverse array of lytic enzymes, including depolymerases, holins, and endolysins, which are capable of breaking down bacterial polysaccharides. This enzymatic action rapidly compromises the structural integrity of biofilms, thereby easing the penetration of phages into the cells located deep within the biofilm layers [9, 48]. In addition to the presence of lysis cassette (Fig. 3a), the halo zones observed in the plaques of phage AB4P2 also suggested that it had the ability to depolymerize exopolysaccharides and destroy biofilms [49]. Structural analysis of the tail fiber protein WPJ20733 identified a pectin lyase-like domain which is associated with depolymerase activity, enabling it to specifically recognize and degrade exopolysaccharides present in biofilms. Typically, biofilm elimination necessitates the synergistic action of multiple phages [50]. For the presence of depolymerase and a lysis cassette, *A. baumannii* phage AB4P2 can significantly reduce the biofilm (52%) even when employed individually. Moreover, phage AB4P2 can effectively killed the live bacterial cells in the biofilm (Fig. 5). Studies have demonstrated that phages can penetrate the biofilm matrix and effectively kill the embedded bacterial cells [51, 52]. Compared to the biofilm elimination rate of *Staphylococcus epidermidis* phage K (about 20–80%), *A. baumannii* phage AB7-IBB1 (35% at MOI 10), *A. baumannii* phages vAbBal23 (about 30%) and vAbAbd25 (up to 68%), phage AB4P2 demonstrates relatively strong efficacy in clearing biofilms [52–54]. Although the biofilm removal efficacy of *A. baumannii* phage vAbAbd25 is better than our phage AB4P2, the bacterial growth completely inhibited by phage vAbAbd25 was kept for four hours, shorter than 16 h by phage AB4P2 [53].

Nosocomial *A. baumannii* infections such as respiratory tract infections, urinary tract infections, and bloodstream infections mainly affect patients with severe underlying disease in the ICU. Respiratory and urinary catheters contamination with *A. baumannii* may be one of the important risk factors [55]. A significant proportion of *A. baumannii* bloodstream infections are related to catheter use [56]. This study utilizes a PVC catheter model to illustrate the formation of biofilms by *A. baumannii* on the catheter surface and their subsequent destruction via phage-induced lysis. Notably, the biofilm developed showed a significant reduction after the exposure to phage AB4P2, with an ablation rate reaching 33% (Fig. 6). These results demonstrated that phage AB4P2 was capable of effectively ablating biofilms in the lab environment and PVC catheter model. Given the excellent biofilm ablation ability of *A. baumannii* by phage AB4P2, it is recommended that hospitals increase the use of phage preparations in intensive care units for the sterilization of *A. baumannii*, thereby reducing the

rate of nosocomial infections. For the absence of any virulence and antimicrobial genes in phage AB4P2, it is also applicable to in-vivo study in the future. In clinical applications, phage therapy has not demonstrated any adverse effects, while simultaneously achieving positive therapeutic outcomes [57–59]. The government departments need to intensify their efforts in promoting phage therapy for clinically drug-resistant bacterial infections in the future.

Conclusion

In conclusion, *A. baumannii* phage AB4P2 isolating from sewage treatment plant water belonged to a new member of *Caudoviricetes* class. With the presence of depolymerase and a lysis cassette, phage AB4P2 had a strong ability to inhibit the growth of *A. baumannii* and destroy formed biofilms by *A. baumannii* on the catheter surface. Despite phage AB4P2 possessing a robust lytic ability, the prolonged use of this phage still led to the emergence of *A. baumannii* AB4 phage-resistant mutants. The quick development of phage resistance is the limitation for the application of single phage. The combination of phage AB4P2 with other phages, antibiotics, and photosensitizer, has the potential to be used as a powerful therapeutic agent and environmental disinfectant for the biological control of infections associated with *A. baumannii* in hospitals. We will continue to pay close attention to the application of phage-based strategies for the control of *A. baumannii* infections in the future, as it holds promising potential in the fight against this persistent threat.

Supplementary Information

The online version contains supplementary material available at https://doi.org/10.1186/s12866-025-03854-3.

Supplementary Material 1: Supplemental Table 1. Host range test for A. baumannii phage vB_AbaM_AB4P2.

Supplementary Material 2: Supplemental Fig. 1 Heatmap of the whole genome ANI values for A. baumannii phage vB_AbaM_AB4P2 and other 19 phages by pyani.

Supplementary Material 3: Supplemental Fig. 2 Percentage sequence similarity between A. baumannii phage vB_AbaM_AB4P2 and other 19 phages using VIDIRIC.

Acknowledgements
We would like to thank doctor Bingshao Liang of Guangzhou Women and Children's Medical Center for providing us with these clinical strains.

Author contributions
JH Su, YJ Tan, SS Liu performed the experiments, analyzed the data, and prepared the initial draft of the manuscript. HH Zou, XY Huang and SY Chen analyzed the data. HM Zhang and ST Li provided important experimental materials. HY Zeng conceived and designed the study, revised the final manuscript.

Funding
This work was supported by the National Natural Science Foundation of China [grant number 32072327].

Data availability
The GenBank accession number of the whole genome sequence of A. baumannii. phage AB4P2 reported in this article is OR544125.

Declarations

Ethics approval and consent to participate
Not applicable. This study was conducted in accordance with local legislation. The water sample was gathered by authorized staff and provided to us with the explicit knowledge and consent of the sewage treatment plant. There was no requirement for a specific permission or license pertaining to the sampling process.

Consent for publication
Not applicable.

Competing interests
The authors declare no competing interests.

Author details
[1]School of Biomedical and Pharmaceutical Sciences, Guangdong University of Technology, Waihuan West Road 100, Guangzhou City, Guangdong Province 510006, China

Received: 16 November 2024 / Accepted: 28 February 2025
Published online: 08 March 2025

References

1. Vázquez-López R, Solano-Gálvez SG, Juárez Vignon-Whaley JJ, Abello Vaamonde JA, Padró Alonzo LA, Rivera Reséndiz A et al. *Acinetobacter baumannii* resistance: A real challenge for clinicians. Antibiot (Basel Switzerland). 2020;9(4).
2. Tagliaferri TL, Jansen M, Horz HP. Fighting pathogenic Bacteria on two fronts: phages and antibiotics as combined strategy. Front Cell Infect Microbiol. 2019;9:22.
3. Gedefie A, Demsis W, Ashagrie M, Kassa Y, Tesfaye M, Tilahun M, et al. *Acinetobacter baumannii* biofilm formation and its role in disease pathogenesis: A review. Infect Drug Resist. 2021;14:3711–9.
4. Law SKK, Tan HS. The role of quorum sensing, biofilm formation, and iron acquisition as key virulence mechanisms in *Acinetobacter baumannii* and the corresponding anti-virulence strategies. Microbiol Res. 2022;260:127032.
5. Tan Y, Su J, Fu M, Zhang H, Zeng H. Recent Advances in Phage-Based Therapeutics for Multi-Drug Resistant *Acinetobacter baumannii*. Bioengineering (Basel, Switzerland). 2023;10(1).
6. Düzgüneş N, Sessevmez M, Yildirim M. Bacteriophage therapy of bacterial infections: the rediscovered frontier. Pharmaceuticals (Basel Switzerland). 2021;14(1).
7. Hibstu Z, Belew H, Akelew Y, Mengist HM. Phage therapy: A different approach to fight bacterial infections. Biologics: Targets Therapy. 2022;16:173–86.
8. Liu S, Lu H, Zhang S, Shi Y, Chen Q. Phages against pathogenic bacterial biofilms and Biofilm-Based infections: A review. Pharmaceutics. 2022;14(2).
9. Pires DP, Oliveira H, Melo LD, Sillankorva S, Azeredo J. Bacteriophage-encoded depolymerases: their diversity and biotechnological applications. Appl Microbiol Biotechnol. 2016;100(5):2141–51.
10. Latka A, Maciejewska B, Majkowska-Skrobek G, Briers Y, Drulis-Kawa Z. Bacteriophage-encoded virion-associated enzymes to overcome the carbohydrate barriers during the infection process. Appl Microbiol Biotechnol. 2017;101(8):3103–19.
11. Liu S, Lei T, Tan Y, Huang X, Zhao W, Zou H, et al. Discovery, structural characteristics and evolutionary analyses of functional domains in *Acinetobacter baumannii* phage tail fiber/spike proteins. BMC Microbiol. 2025;25(1):73.
12. Islam MM, Mahbub NU, Shin WS, Oh MH. Phage-encoded depolymerases as a strategy for combating multidrug-resistant *Acinetobacter baumannii*. Front Cell Infect Microbiol. 2024;14.

13. Ferriol-Gonzalez C, Domingo-Calap P. Phages for biofilm removal. Antibiot (Basel). 2020;9(5).
14. Lu TK, Collins JJ. Dispersing biofilms with engineered enzymatic bacteriophage. Proc Natl Acad Sci U S A. 2007;104(27):11197–202.
15. Guo Z, Liu M, Zhang D. Potential of phage depolymerase for the treatment of bacterial biofilms. Virulence. 2023;14(1):2273567.
16. Ahmad TA, Houjeiry SE, Kanj SS, Matar GM, Saba ES. From forgotten cure to modern medicine: the resurgence of bacteriophage therapy. J Glob Antimicrob Resist. 2024;39:231–9.
17. Lin J, Du F, Long M, Li P. Limitations of phage therapy and corresponding optimization strategies: A review. Molecules. 2022;27(6).
18. Malik DJ, Sokolov IJ, Vinner GK, Mancuso F, Cinquerrui S, Vladisavljevic GT, et al. Formulation, stabilisation and encapsulation of bacteriophage for phage therapy. Adv Colloid Interface Sci. 2017;249:100–33.
19. Strathdee SA, Hatfull GF, Mutalik VK, Schooley RT. Phage therapy: from biological mechanisms to future directions. Cell. 2023;186(1):17–31.
20. Tan Y, Su J, Luo D, Liang B, Liu S, Zeng H. Isolation and genome-wide analysis of the novel *Acinetobacter baumannii* bacteriophage vB_AbaM_AB3P2. Arch Virol. 2024;169(3):66.
21. Zhang Z, Liang L, Li D, Li Y, Sun Q, Li Y, et al. Bacillus subtilis phage phi18: genomic analysis and receptor identification. Arch Virol. 2023;168(1):17.
22. Zeng H, Li C, Luo D, Zhang J, Ding Y, Chen M, et al. Novel phage vB_CtuP_B1 for controlling *Cronobacter malonaticus* and *Cronobacter turicensis* in ready-to-eat lettuce and powered infant formula. Food Res Int. 2021;143:110255.
23. Duan S, Dong Y, Xu Y, Yin J, Geng L, Xiu Z. One-step salting-out extraction of bacteriophage from its infection broth of *Acinetobacter baumannii*. J Chromatogr A. 2022;1679:463407.
24. Yang Z, Liu X, Shi Y, Yin S, Shen W, Chen J, et al. Characterization and genome annotation of a newly detected bacteriophage infecting multidrug-resistant *Acinetobacter baumannii*. Arch Virol. 2019;164(6):1527–33.
25. Bankevich A, Nurk S, Antipov D, Gurevich AA, Dvorkin M, Kulikov AS, et al. SPAdes: a new genome assembly algorithm and its applications to single-cell sequencing. J Comput Biology: J Comput Mol Cell Biology. 2012;19(5):455–77.
26. Jiang JZ, Yuan WG, Shang J, Shi YH, Yang LL, Liu M et al. Virus classification for viral genomic fragments using PhaGCN2. Brief Bioinform. 2023;24(1).
27. Price MN, Dehal PS, Arkin AP. FastTree: computing large minimum evolution trees with profiles instead of a distance matrix. Mol Biol Evol. 2009;26(7):1641–50.
28. Moraru C, Varsani A, Kropinski AM. VIRIDIC-A novel tool to calculate the intergenomic similarities of Prokaryote-Infecting viruses. Viruses. 2020;12(11).
29. Sullivan MJ, Petty NK, Beatson SA. Easyfig: a genome comparison visualizer. Bioinformatics. 2011;27(7):1009–10.
30. Paysan-Lafosse T, Blum M, Chuguransky S, Grego T, Pinto BL, Salazar GA, et al. InterPro in 2022. Nucleic Acids Res. 2023;51(D1):D418–27.
31. Abramson J, Adler J, Dunger J, Evans R, Green T, Pritzel A et al. Accurate structure prediction of biomolecular interactions with alphafold 3. Nature. 2024:1–3.
32. DeLano WL, et al. Pymol: an open-source molecular graphics tool. CCP4 Newsl Protein Crystallogr. 2002;40(1):82–92.
33. Ran B, Yuan Y, Xia W, Li M, Yao Q, Wang Z, et al. A photo-sensitizable phage for multidrug-resistant *Acinetobacter baumannii* therapy and biofilm ablation. Chem Sci. 2020;12(3):1054–61.
34. Childers C, Edsall C, Gannon J, Whittington AR, Muelenaer AA, Rao J et al. Focused ultrasound biofilm ablation: investigation of histotripsy for the treatment of Catheter-Associated urinary tract infections (CAUTIs). IEEE transactions on ultrasonics, ferroelectrics, and frequency control. 2021;68(9):2965–80.
35. Fu W, Forster T, Mayer O, Curtin JJ, Lehman SM, Donlan RM. Bacteriophage cocktail for the prevention of biofilm formation by *Pseudomonas aeruginosa* on catheters in an in vitro model system. Antimicrob Agents Chemother. 2010;54(1):397–404.
36. Liu Y, Mi L, Mi Z, Huang Y, Li P, Zhang X et al. Complete Genome Sequence of IME207, a Novel Bacteriophage Which Can Lyse Multidrug-Resistant *Klebsiella pneumoniae* and *Salmonella*. Genome announcements. 2016;4(5).
37. Liu Y, Mi Z, Mi L, Huang Y, Li P, Liu H, et al. Identification and characterization of capsule depolymerase Dpo48 from *Acinetobacter baumannii* phage IME200. PeerJ. 2019;7:e6173.
38. Gutiérrez D, Martínez B, Rodríguez A, García P. Genomic characterization of two *Staphylococcus epidermidis* bacteriophages with anti-biofilm potential. BMC Genomics. 2012;13:1–10.
39. Peters DL, Gaudreault F, Chen W. Functional domains of *Acinetobacter* bacteriophage tail fibers. Front Microbiol. 2024;15:1230997.
40. Cai X, Tian J, Zhu J, Chen J, Li L, Yang C, et al. Photodynamic and photothermal co-driven CO-enhanced multi-mode synergistic antibacterial nanoplatform to effectively fight against biofilm infections. Chem Eng J. 2021;426:131919.
41. Dai X, Yu Y, Wei X, Dai X, Duan X, Yu C, et al. Peptide-Conjugated CuS nanocomposites for NIR-Triggered ablation of *Pseudomonas aeruginosa* biofilm. ACS Appl Bio Mater. 2019;2(4):1614–22.
42. Sisakhtpour B, Mirzaei A, Karbasizadeh V, Hosseini N, Shabani M, Moghim S. The characteristic and potential therapeutic effect of isolated multidrug-resistant *Acinetobacter baumannii* lytic phage. Ann Clin Microbiol Antimicrob. 2022;21(1):1.
43. Mardiana M, Teh SH, Lin LC, Lin NT. Isolation and characterization of a novel siphoviridae phage, vB_AbaS_TCUP2199, infecting Multidrug-Resistant *Acinetobacter baumannii*. Viruses. 2022;14(6).
44. Wintachai P, Surachat K, Singkhamanan K. Isolation and characterization of a novel autographiviridae phage and its combined effect with Tigecycline in controlling Multidrug-Resistant *Acinetobacter baumannii*-Associated skin and soft tissue infections. Viruses. 2022;14(2).
45. Choi Y, Kwak MJ, Kang MG, Kang AN, Lee W, Mun D, et al. Molecular characterization and environmental impact of newly isolated lytic phage SLAM_phiST1N3 in the Cornellvirus genus for biocontrol of a multidrug-resistant *Salmonella Typhimurium* in the swine industry chain. Sci Total Environ. 2024;922:171208.
46. Kamyab H, Torkashvand N, Shahverdi AR, Khoshayand MR, Sharifzadeh M, Sepehrizadeh Z. Isolation, characterization, and genomic analysis of vB_PaeP_TUMS_P121, a new lytic bacteriophage infecting *Pseudomonas aeruginosa*. Arch Virol. 2022;168(1):8.
47. Lucidi M, Visaggio D, Migliaccio A, Capecchi G, Visca P, Imperi F, et al. Pathogenicity and virulence of *Acinetobacter baumannii*: factors contributing to the fitness in healthcare settings and the infected host. Virulence. 2024;15(1):2289769.
48. Topka-Bielecka G, Dydecka A, Necel A, Bloch S, Nejman-Falenczyk B, Wegrzyn G et al. Bacteriophage-Derived depolymerases against bacterial biofilm. Antibiot (Basel Switzerland). 2021;10(2).
49. Islam MS, Raz A, Liu Y, Elbassiony KRA, Dong X, Zhou P et al. Complete genome sequence of *Aeromonas* phage ZPAH7 with halo zones, isolated in China. Microbiol Resour Announc. 2019;8(10).
50. Byun KH, Han SH, Choi MW, Kim BH, Park SH, Ha SD. Biofilm eradication ability of phage cocktail against *Listeria monocytogenes* biofilms formed on food contact materials and effect on virulence-related genes and biofilm structure. Food Res Int. 2022;157:111367.
51. Kay MK, Erwin TC, McLean RJ, Aron GM. Bacteriophage ecology in *Escherichia coli* and *Pseudomonas aeruginosa* mixed-biofilm communities. Appl Environ Microbiol. 2011;77(3):821–9.
52. Cerca N, Oliveira R, Azeredo J. Susceptibility of *Staphylococcus epidermidis* planktonic cells and biofilms to the lytic action of *staphylococcus* bacteriophage K. Lett Appl Microbiol. 2007;45(3):313–7.
53. Ndiaye I, Debarbieux L, Sow O, Ba BS, Diagne MM, Cissé A, et al. Characterization of two *Friunavirus* phages and their inhibitory effects on biofilms of extremely drug resistant *Acinetobacter baumannii* in Dakar, Senegal. BMC Microbiol. 2024;24(1):449.
54. Yele AB, Thawal ND, Sahu PK, Chopade BA. Novel lytic bacteriophage AB7-IBB1 of *Acinetobacter baumannii*: isolation, characterization and its effect on biofilm. Arch Virol. 2012;157(8):1441–50.
55. Bustamante V, Palavecino CE. Effect of photodynamic therapy on multidrug-resistant *Acinetobacter baumannii*: A scoping review. Photodiagn Photodyn Ther. 2023;43:103709.
56. Zhang S, Sun L, Sun L, Yang Z. [Application progress of polymyxin in bloodstream infection of drug-resistant *Acinetobacter baumannii*]. Zhonghua Wei Zhong Bing Ji Jiu Yi Xue. 2021;33(11):1401–4.
57. Schooley RT, Biswas B, Gill JJ, Hernandez-Morales A, Lancaster J, Lessor L et al. Development and use of personalized Bacteriophage-Based therapeutic cocktails to treat a patient with a disseminated resistant *Acinetobacter baumannii* infection. Antimicrob Agents Chemother. 2017;61(10).
58. Tan X, Chen H, Zhang M, Zhao Y, Jiang Y, Liu X, et al. Clinical experience of personalized phage therapy against Carbapenem-Resistant *Acinetobacter baumannii* lung infection in a patient with chronic obstructive pulmonary disease. Front Cell Infect Microbiol. 2021;11:631585.

59. Wang WX, Wu JZ, Zhang BL, Yu JY, Han LM, Lu XL, et al. Phage therapy combats pan drug-resistant *Acinetobacter baumannii* infection safely and efficiently. Int J Antimicrob Agents. 2024;64(2):107220.

Publisher's note